Journal of Luminescence 142 (2013) 196–201

Contents lists available at SciVerse ScienceDirect

Journal of Luminescence

journal homepage: www.elsevier.com/locate/jlumin

Enhancement of electron transfer from CdSe core/shell quantum dots to TiO_2 films by thermal annealing

Cong Shao [a,b], Xiangdong Meng [c], Pengtao Jing [a], Mingye Sun [a,b], Jialong Zhao [a,c,*], Haibo Li [c,**]

[a] State Key Laboratory of Luminescence and Applications, Changchun Institute of Optics, Fine Mechanics and Physics, Chinese Academy of Sciences, 3888 Eastern South Lake Road, Changchun 130033, China
[b] University of Chinese Academy of Sciences, Beijing 100039, China
[c] Key Laboratory of Functional Materials Physics and Chemistry of the Ministry of Education, Jilin Normal University, Siping 136000, China

ARTICLE INFO

Article history:
Received 19 December 2012
Received in revised form
3 April 2013
Accepted 9 April 2013
Available online 18 April 2013

Keywords:
CdSe
Quantum dots
Nanocrystals
Electron transfer
Thermal annealing

ABSTRACT

We demonstrated the enhancement of electron transfer from CdSe/ZnS core/shell quantum dots (QDs) to TiO_2 films via thermal annealing by means of steady-state and time-resolved photoluminescence (PL) spectroscopy. The significant decrease in PL intensities and lifetimes of the QDs on TiO_2 films was clearly observed after thermal annealing at temperature ranging from 100 °C to 300 °C. The obtained rates of electron transfer from CdSe core/shell QDs with red, yellow, and green emissions to TiO_2 films were significantly enhanced from several times to an order of magnitude (from ~10^7 s^{-1} to ~10^8 s^{-1}). The improvement in efficiencies of electron transfer in the TiO_2/CdSe QD systems was also confirmed. The enhancement could be considered to result from the thermal annealing reduced distance between CdSe QDs and TiO_2 films. The experimental results revealed that thermal annealing would play an important role on improving performances of QD based optoelectronic devices.

1. Introduction

Colloidal quantum dots (QDs) have been used as light harvesting components in their sensitized solar cells (SSC) due to their size-tunable band gap and low-cost solution fabrication [1–3]. The observation of multiple exciton generation in QDs opens the possibility of boosting the energy conversion efficiency of QDSSCs to exceed the traditional thermodynamic limit for single junction bulk SCs [4,5]. However, currently the maximum power conversion efficiency of the QDSSCs is still lower than 5%, which is dependent on the generation efficiency of electron–hole pairs (excitons), charge transfer dynamics, and electron recombination processes in the devices [3–7].

The dynamic processes of electron transfer between CdSe QDs and the metal oxides such as TiO_2 have been extensively studied for understanding the improvement in performances of QDSSCs in the past two decades. Robel et al. determined electron transfer rate in TiO_2/CdSe QD system in the range from 1.2×10^{10} s^{-1} for 2.4 nm QDs to 9.6×10^7 s^{-1} for 7.5 nm QDs and found that the rate was strongly dependent on the dot size [8–10]. Tvrdy et al. systematically studied the dependence of electron transfer rate constants from CdSe QD donors to metal oxide nanoparticle acceptors (TiO_2, ZnO, and SnO_2) on the change in system free energy [11]. Shen et al. observed that the performance of TiO_2/CdSe QD based solar cells was improved by coating a ZnS shell or a CdS shell on CdSe nanocrystals to reduce recombination processes at the interface of the metal oxide/QD or passivate the electron traps for the enhancement of the electron transfer efficiency [12–16]. Further CdSe/ZnS core/shell QDs on an anatase electrode surface in an aqueous iodide electrolyte exhibited relative long photocurrent stability, compared to CdSe cores [17]. Similarly, surface defect states resulting from the removal of capping molecules can be passivated by growing a thin ZnS or CdS shell on the CdSe core, greatly enhancing the photoconductivity of QD films and photostability of QDs [18–20]. Despite the inorganic shell as an energetic barrier for electron transfer, the relatively large average electron transfer rate from CdSe/ZnS (4.0 nm) core/shell QDs to TiO_2 was estimated to be 3.2×10^7 s^{-1} [21]. In addition, the electron transfer rate of CdSe/CdS core/shell QDs into a TiO_2 substrate was also measured to be 8.1×10^8 s^{-1} [16]. As a result, the electron transfer processes are greatly dependent on the distance between the QD and TiO_2.

It is known that thermal annealing can remove the organic surfactants from the surface of QDs for reducing the distance and consequently increasing the electronic coupling between the QDs.

* Corresponding author. Tel.: +86 431 86176313.
** Also corresponding author. Tel.: +86 434 3290232.
E-mail addresses: zhaojl@ciomp.ac.cn, jlzhaoqd@yahoo.com (J. Zhao), lihaibo@jlnu.edu.cn (H. Li).

0022-2313/$ - see front matter © 2013 Elsevier B.V. All rights reserved.
http://dx.doi.org/10.1016/j.jlumin.2013.04.005

Post heat treatment processes have significantly influenced optical and electrical properties of the QD films and improved the performance of QD based optoelectronic devices [1,2,18–20, 22–28]. The red or blue shift of the absorption bands and PL peaks for the CdSe core and core/shell QDs was observed in their solid films, which was related to the aggregation of dots, changes in the size and shape distribution, and reduction in interdot separation [18,27–33]. In particular, the degradation in the photoluminescence (PL) properties of QDs was considered to result from the formation of surface defect states as non-radiative recombination centers on the surface of the QDs due to the loss of surface ligands during the heat treatment [29–33]. The semiconductor shell-coated CdSe QDs were found to exhibit more superior thermal stability than their core QDs [32,33]. Therefore, it is very important to understand the effect of thermal annealing on electron transfer processes from CdSe/ZnS core/shell QDs to TiO_2 films for designing high quality QDSSCs.

In this work, we report the thermal annealing effect on the rate and efficiency of electron transfer from CdSe/ZnS and CdSe/CdS/ZnS core/shell QDs to TiO_2 films by using steady-state and time-resolved PL spectroscopy. The rate and efficiency of electron transfer from the QDs to TiO_2 films estimated based on the change in PL lifetimes of the QDs on TiO_2 and SiO_2 films annealed at various temperatures ranging from 100 °C to 300 °C in nitrogenous atmosphere are compared with those of the metal oxide/QD systems without annealing. The enhancement of the electron transfer in TiO_2/CdSe QD systems via thermal annealing is discussed in detail.

2. Experimental section

2.1. NC synthesis

CdSe/ZnS and CdSe/CdS/ZnS core/shell QDs with various core diameters and shell thicknesses were synthesized via a hot injection method described in Ref. [34]. The CdSe/ZnS core/shell QDs were obtained by the growth of 2–3 monolayers (MLs) of ZnS shells on the CdSe core. The CdSe/CdS/ZnS core/multishell QDs were obtained by the growth of 2–4 MLs of CdS and 2–3 MLs of ZnS shells on the CdSe core. After synthesis, the surface ligands (either oleic acid, or TOPO) were exchanged with dodecanthiol ($CH_3(CH_2)_{11}SH$). TiO_2 nanocrystals were synthesized via a two-phase thermal route with narrow size distribution described in Ref. [35]. SiO_2 nanoparticles were obtained by a method described in Ref. [36].

2.2. Preparation of metal oxide/QD systems

TiO_2 and SiO_2 films were prepared by spin-coating these nanocrystals with high concentration in toluene or ethanol onto glass substrates with a speed of 1500 rpm for 30 s, sintered at a temperature of 450 °C in air for 30 min, and then cooled to room temperature naturally for the formation of surfactant free and relatively flat nanocrystal films. After that, CdSe core/multishell QD solutions with very low concentration were spun onto the metal oxide films, preventing the aggregation of the QDs on the TiO_2 and SiO_2 films. These TiO_2/CdSe and SiO_2/CdSe QD samples were annealed at temperature ranging from 100 °C to 300 °C with an interval of 50 °C for 10 min in nitrogenous atmosphere.

2.3. Optical characterization

The absorption spectra were recorded by a UV-3101PC UV–vis–NIR scanning spectrophotometer (Shimadzu). Fluorescence and excitation spectra of the colloidal QDs in solution were recorded by a Hitachi F-4500 spectrophotometer equipped with a 150 W Xe-arc lamp. The PL spectra of the QDs on oxide films were dispersed by a monochromator and detected by a Jobin–Yvon Si-CCD under excitation of a 488 nm line from an Ar^+ laser. The laser beam was focused onto the samples by a magnification microscope objective (10×, N.A.=0.25). The time resolved PL spectra were measured by LifeSpec-II Dedicated Lifetime Spectrometer (Edinburgh Instruments). The excitation sources were picosecond pulsed diode lasers with a laser wavelength of 405 and 485 nm, respectively. The transmission electron microscopy (TEM) images were recorded in a Philips TECNAI G2 operated at an accelerating voltage of 200 kV. The surfaces of the inorganic nanocrystal films were measured using Hitachi S4800 scanning electron microscope (SEM) equipped with a field emission gun operated at 10 kV. All measurements were carried out at room temperature.

3. Results and discussion

Fig. 1 shows absorption and PL spectra of typical red CdSe/CdS/ZnS core/multishell and green CdSe/ZnS core/shell QDs. The red CdSe QDs with an average diameter of 7.5 nm were prepared by growing 4 ML CdS and 2.5 ML ZnS shells on the surface of the large CdSe core with a diameter of 3.0 nm and an emission of 548 nm. The green CdSe QDs with an average diameter of 4.1 nm were obtained by growing a 3 ML ZnS shell on the surface of the small CdSe core with a diameter of 2.6 nm and an emission of 533 nm. The absorption spectrum of TiO_2 nanocrystals in toluene is also shown in the figure. As seen in Fig. 1, the red QDs have the first excitonic absorption band at 607 nm and a band edge PL peak at 618 nm while the green QDs exhibit the first excitonic absorption band at 522 nm and a PL peak at 536 nm. The TiO_2 film on glass is transparent in the ultraviolet–visible region. Tvrdy et al. demonstrated photoinduced electron transfer from CdSe core QDs to TiO_2 films with the conduction band position of −4.41 eV (vs. vacuum) as an electron acceptor and conductor. The differently sized CdSe QDs with the conduction levels between −3.65 and −3.94 eV (vs. vacuum) can be an electron donor [11]. Therefore, the electron transfer from CdSe core QDs to TiO_2 films is energetically allowable. Further, because SiO_2 is an insulator, it cannot act as an

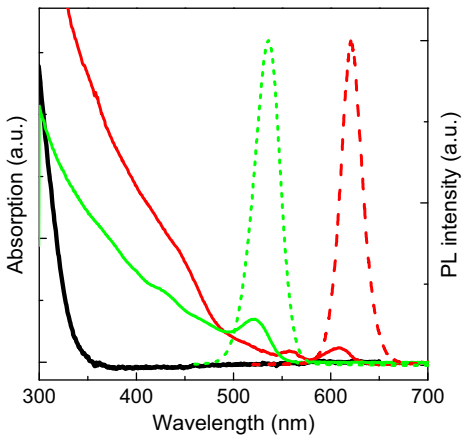

Fig. 1. Absorption (solid lines) and PL (dashed lines) spectra of red CdSe/CdS/ZnS (red lines) and green CdSe/ZnS core/shell QDs (green lines). Absorption and PL spectra were taken from the QDs in chloroform and on SiO_2 films, respectively. The excitation wavelength is 450 nm. The thick black line represents the absorption spectrum of TiO_2 nanocrystals in toluene. (For interpretation of the references to color in this figure legend, the reader is referred to the web version of this article.)

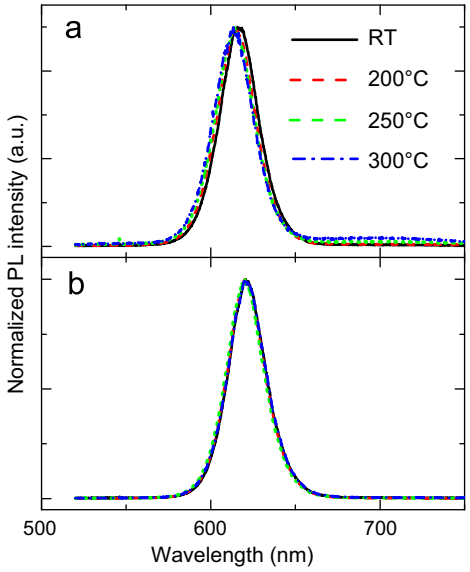

Fig. 2. Normalized PL spectra of red CdSe/CdS/ZnS core/multishell QDs on TiO_2 (a) and SiO_2 (b) films. The excitation wavelength is 488 nm. The black (solid), red (dash), green (short dash) and blue (dash dot) lines represent the PL spectra of the QDs without annealing (room temperature (RT)) and with annealing temperature of 200, 250, and 300 °C, respectively. (For interpretation of the references to color in this figure legend, the reader is referred to the web version of this article.)

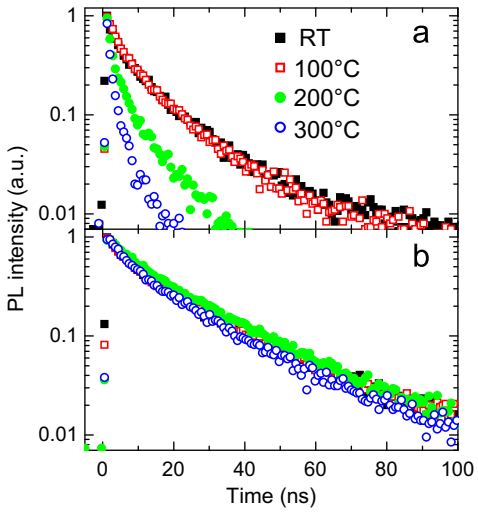

Fig. 3. PL decay curves of red CdSe/CdS/ZnS core/mulitshell QDs on TiO_2 (a) and SiO_2 (b) films at various annealing temperature. The Excitation wavelength is 485 nm. The monitor wavelength is 618 nm. The black solid squares, red empty squares, green solid circles, and blue empty circles represent the PL spectra of the QDs without annealing and with annealing temperature of 100, 200, and 300 °C, respectively. (For interpretation of the references to color in this figure legend, the reader is referred to the web version of this article.)

electron acceptor. As a result, we can measure the electron transfer from CdSe QDs to TiO_2 films by using CdSe QDs on SiO_2 films as reference samples under various thermal annealing temperatures [8–11].

The PL spectra of CdSe/CdS/ZnS core/multishell QDs on TiO_2 and SiO_2 films annealed at various temperatures are shown in Fig. 2. It is found that the PL intensity of the red QDs on TiO_2 films is significantly reduced while no clear change in PL intensity of the QDs on SiO_2 films is confirmed after thermal annealing. No clear defect/trap state-related emission band around 700 nm is observed for the QDs on TiO_2 and SiO_2 films annealed at high temperatures. In the experiment, we are not able to absolutely measure the intensities of QD samples under different temperature for comparison but we can exactly determine their PL lifetimes. Therefore we will study the electron transfer from the QDs to TiO_2 by measuring PL lifetimes of QDs on TiO_2 and SiO_2 films.

In order to quantify the electron transfer dynamics of red and green CdSe/CdS/ZnS core/multishell QDs on the oxide films, we selected the excitation wavelength of 485 and 405 nm, which is below the absorption edge of TiO_2 films. Fig. 3 shows the PL decay curves of red CdSe/CdS/ZnS core/multishell QDs on TiO_2 and SiO_2 films at various annealing temperatures. As seen in Fig. 3a, the PL decay of the QDs on TiO_2 films becomes significantly faster with increasing the annealing temperature in contrast to that of the QDs on SiO_2 films annealed at the same condition, resulting from an enhanced electron transfer process from the QDs to TiO_2 films [10]. As seen in Fig. 3b, the PL decay curves of the red CdSe core/multishell QDs on SiO_2 films do not show any clear change after thermal annealing, which is consistent with that of their PL intensity. This indicates that the red QDs with a thicker multishell are very thermally stable, confirming that the as-prepared red CdSe/CdS/ZnS core/multishell QDs are high quality luminescent nanocrystals.

The decay curves of the red CdSe/CdS/ZnS core/multishell QDs were fitted with a triexponential function: $I(t)=A_1\exp(-t/\tau_1)+A_2\exp(-t/\tau_1)+A_3\exp(-t/\tau_1)$, where A_1, A_2, and A_3 are fractional contributions of decay lifetimes τ_1, τ_2, and τ_3, respectively. The average lifetime τ_{ave} can be determined by an expression:

Table 1
Time constants, the normalized amplitudes of the components, average lifetimes of photoluminescence for red-CdSe/TiO_2 and red-CdSe/SiO_2 samples. The rates of electron transfer between CdSe and TiO_2 are given in the table.

Samples	A_1	τ_1 (ns)	A_2	τ_2 (ns)	A_3	τ_3 (ns)	τ_{ave} (ns)	k_{ET} (10^7 s^{-1})
TiO_2/CdSe 20 °C	0.31	1.25	0.48	6.86	0.20	20.13	13.44	3.01
TiO_2/CdSe 100 °C	0.33	1.72	0.49	7.50	0.17	20.53	12.99	3.42
TiO_2/CdSe 150 °C	0.55	1.33	0.39	5.73	0.10	18.03	9.83	5.69
TiO_2/CdSe 200 °C	0.72	1.14	0.31	5.56	0.04	18.14	7.47	9.15
TiO_2/CdSe 250 °C	0.90	1.20	0.17	6.81	0.02	17.41	6.26	11.70
TiO_2/CdSe 300 °C	0.49	1.03	0.55	1.12	0.09	7.029	3.27	25.67
SiO_2/CdSe 20 °C	0.30	3.88	0.45	14.18	0.23	32.54	22.58	
SiO_2/CdSe 100 °C	0.31	3.74	0.46	14.32	0.22	34.41	23.39	
SiO_2/CdSe 150 °C	0.26	3.05	0.48	11.70	0.28	31.08	22.34	
SiO_2/CdSe 200 °C	0.26	4.83	0.60	18.53	0.14	38.79	23.58	
SiO_2/CdSe 250 °C	0.10	1.68	0.40	10.12	0.49	27.63	23.39	
SiO_2/CdSe 300 °C	0.28	4.00	0.47	13.63	0.23	29.39	20.37	

$\tau_{ave}=(A_1\tau_1^2+A_2\tau_2^2+A_3\tau_3^3)/(A_1\tau_1+A_2\tau_2+A_3\tau_3)$. The average lifetimes of the red QDs on TiO_2 and SiO_2 films without thermal annealing were determined to be 13.44 and 22.58 ns, respectively, as seen in Table 1. The average lifetime of the QDs on TiO_2 films is clearly shorter than that of the QDs on the SiO_2 film, indicating that electron transfer from the CdSe QDs to TiO_2 films is an added de-excitation pathway for the QDs. Considering that no electron transfer happens between the QDs on SiO_2 film, we can calculate the electron transfer rate and efficiency from the QDs to TiO_2 films using relations [11]: $k_{ET}=1/\tau_{ave}(QD/TiO_2)-1/\tau_{ave}(QD/SiO_2)$ and $\eta_{ET}=1-\tau_{ave}(QD/TiO_2)/\tau_{ave}(QD/SiO_2)$, here $\tau_{ave}(QD/TiO_2)$ and $\tau_{ave}(QD/SiO_2)$ are the average PL lifetimes of the QDs on TiO_2 and SiO_2 films, respectively. The electron transfer rate and efficiency from the red CdSe core/multishell QDs to TiO_2 films without annealing were calculated to be 3.01×10^7 s^{-1} and 41%, respectively. The obtained electron transfer rate is much smaller than that from CdSe core QDs to TiO_2 films [8–11], but is consistent with that from CdSe/ZnS core/shell QDs to a TiO_2 film [21]. The average lifetimes of the CdSe/CdS/ZnS core/multishell QDs on TiO_2 and SiO_2 films annealed at various temperatures are shown in Fig. 4a. It is noted the PL lifetime of the red CdSe core/multishell QDs on

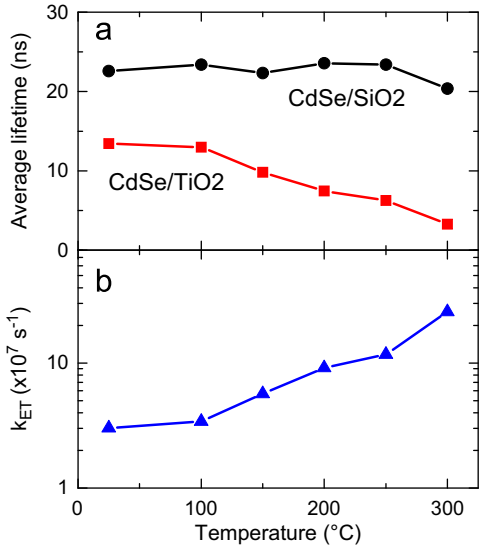

Fig. 4. (a) The average PL lifetime of red CdSe/CdS/ZnS core/multishell QDs on TiO_2 (solid squares) and SiO_2 (solid circles) films without annealing and with annealing; (b) electron transfer rate from the QDs to TiO_2 films as a function of thermal annealing temperature. Lines are guides to eyes.

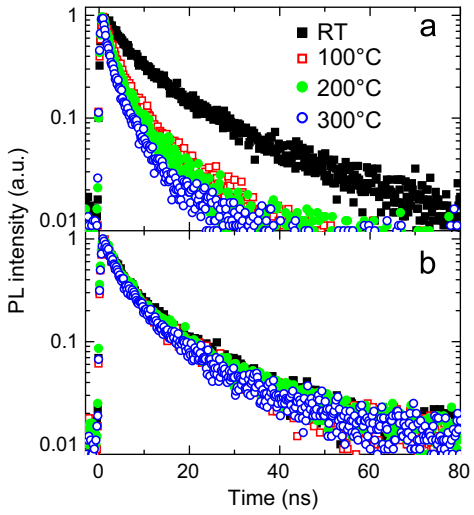

Fig. 5. The PL decay curves of green CdSe/ZnS core/shell QDs on TiO_2 (a) and SiO_2 (b) films at various annealing temperatures. Excitation wavelength is 405 nm. The monitor wavelength is 536 nm. The black solid squares, red empty squares, green solid circles, and blue empty circles represent the PL spectra of the QDs without annealing and with annealing at temperature 100, 200, and 300 °C, respectively. (For interpretation of the references to color in this figure legend, the reader is referred to the web version of this article.)

TiO_2 films is significantly dependent on the thermal annealing temperature. The PL lifetime of the CdSe QDs significantly decreases from 13.44 ns to 3.27 ns for the QDs on the TiO_2 film when the annealing temperature increases from 100 °C to 300 °C. This results in a significant increase in the rate of the electron transfer from 3.01×10^7 s^{-1} to 2.57×10^8 s^{-1} and the efficiency of the electron transfer from 41% to 84% for the TiO_2/CdSe QD system in the annealing temperature range as shown in Fig. 4b. This indicates that the electron transfer rate and efficiency from the CdSe core/multishell QDs to TiO_2 films can be effectively improved via thermal annealing.

Further the green CdSe/ZnS core/shell QDs (4.1 nm) on TiO_2 and SiO_2 films were annealed at various temperatures. It was found that the PL intensity of the QDs on TiO_2 films decreased with increasing the annealing temperature. No clear shift in the peak of the band edge PL was observed for the QDs on the films because the diluted QD solutions were deposited on the oxide films for preventing QD aggregation to quench the PL of the QDs [32,33]. Fig. 5 shows the PL decay curves of the green CdSe/ZnS core/shell QDs on TiO_2 and SiO_2 films annealed at various temperatures. The PL decays of the QDs on TiO_2 films are significantly shortened with increasing the annealing temperature. At the same time, the PL decay curves of the QDs on SiO_2 films shows a small change after thermal annealing. The average lifetimes of the green CdSe/ZnS core/shell QDs on TiO_2 and SiO_2 films without thermal annealing were determined to be 8.75 and 14.74 ns, respectively. The shortening of the PL lifetime is considered to result from the electron transfer from the QDs to TiO_2.

Fig. 6 shows the average lifetimes of the green CdSe/ZnS core/shell QDs on TiO_2 and SiO_2 films annealed at various temperatures and rates of the electron transfer from the QDs to TiO_2 as a function of annealing temperature. The PL lifetime of the QDs on TiO_2 films is significantly shortened with increasing the annealing temperature as seen in Table 2. As seen in Fig. 6a, the PL lifetime of the QDs on TiO_2 is shortened from 7.73 to 6.16 ns at annealing temperature ranging from 100 °C to 300 °C. The estimated electron transfer rate and efficiency from the QDs to TiO_2 films is only enhanced from 4.64×10^7 s^{-1} to 9.01×10^7 s^{-1} and 43% to 56%, respectively, as shown in Fig. 6b. Therefore, the electron transfer rate and efficiency of the green CdSe/ZnS core/shell QDs into TiO_2 films is clearly enhanced via thermal annealing.

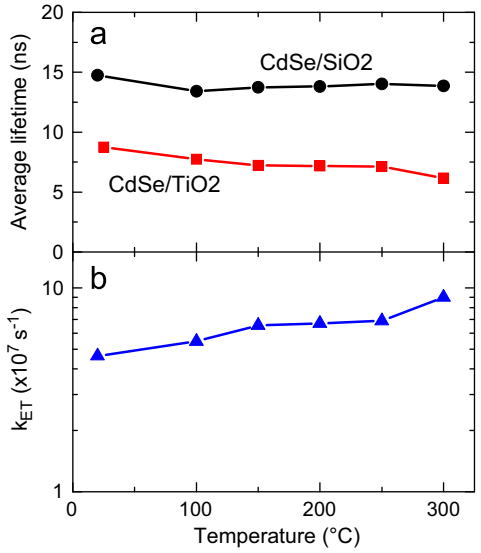

Fig. 6. (a) The average PL lifetime of green CdSe/ZnS core/shell QDs on TiO_2 (solid squares) and SiO_2 (solid circles) films without annealing and with annealing; (b) electron transfer rate from the QDs to TiO_2 films as a function of thermal annealing temperature. Lines are guides to eyes.

In addition, we also studied the improvement of electron transfer for CdSe/ZnS core/shell QDs with thermal instability. Fig. 7 shows the PL decay curves of the yellow CdSe/ZnS core/shell QDs with a 2 ML ZnS shell on TiO_2 and SiO_2 films. It is found that the PL lifetime of the QDs on SiO_2 films significantly decreases with increasing annealing temperature which may result from the formation of amount of surface defect/trap states on the surface of the QDs as nonradiative recombination centers due to removal of ligands on the QD surface under thermal annealing at high temperatures. This also means that the QDs are unstable despite the coating of a thin ZnS shell on the QD. The average lifetimes of the QDs on TiO_2 and SiO_2 films without thermal annealing were determined to be 8.14 and 11.39 ns, respectively. The rate and efficiency of the electron transfer rate were enhanced from

Table 2
Time constants, the normalized amplitudes of the components, average lifetimes of photoluminescence for green-CdSe/TiO_2 and green-CdSe/SiO_2 samples. The rates of electron transfer between CdSe and TiO_2 are given in the table.

Samples	A_1	τ_1 (ns)	A_2	τ_2 (ns)	A_3	τ_3 (ns)	τ_{ave} (ns)	k_{ET} (10^7 s^{-1})
TiO_2/CdSe 20 °C	0.51	2.08	0.42	6.65	0.06	19.73	8.75	4.64
TiO_2/CdSe 100 °C	0.62	2.00	0.34	6.34	0.04	20.20	7.73	5.47
TiO_2/CdSe 150 °C	0.54	1.75	0.39	5.05	0.07	15.78	7.23	6.56
TiO_2/CdSe 200 °C	0.64	1.74	0.30	5.52	0.05	17.33	7.17	6.70
TiO_2/CdSe 250 °C	0.43	1.12	0.43	4.04	0.09	13.77	7.13	6.89
TiO_2/CdSe 300 °C	0.68	1.26	0.28	4.74	0.03	17.69	6.16	9.01
SiO_2/CdSe 20 °C	0.36	3.32	0.47	9.17	0.12	26.61	14.74	
SiO_2/CdSe 100 °C	0.48	2.50	0.42	7.97	0.09	26.49	13.41	
SiO_2/CdSe 150 °C	0.52	2.91	0.38	9.13	0.06	31.13	13.75	
SiO_2/CdSe 200 °C	0.43	2.32	0.44	7.43	0.11	25.32	13.80	
SiO_2/CdSe 250 °C	0.53	2.56	0.37	8.56	0.08	28.48	14.0	
SiO_2/CdSe 300 °C	0.51	2.61	0.38	8.30	0.08	28.26	13.85	

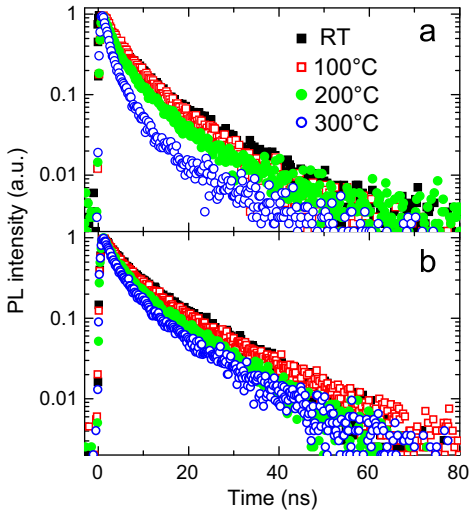

Fig. 7. The PL decay curves of yellow CdSe/ZnS core/shell QDs on TiO_2 (a) and SiO_2 (b) films at various annealing temperatures. Excitation wavelength is 405 nm. The monitor wavelength is 578 nm. The black solid squares, red empty squares, green solid circles, and blue empty circles represent the PL spectra of the QDs without annealing and with annealing at temperature 100, 200, and 300 °C, respectively. (For interpretation of the references to color in this figure legend, the reader is referred to the web version of this article.)

3.5×10^7 s^{-1} to 1.08×10^8 s^{-1} and from 29% to 46%, respectively, with varying the temperature from 100 °C to 300 °C. Therefore, thermal annealing can also clearly enhance the electron transfer process in the TiO_2/CdSe QD system with unstable QDs.

A schematic diagram of the conduction (CB) and valence bands (VB), structures of the CdSe/CdS/ZnS core/multishell QDs, TiO_2 film, and the highest occupied molecular orbital (HOMO) and the lowest unoccupied molecular orbital (LUMO) levels of the organic ligands is shown in Fig. 8. We have found that the rates of the electron transfer from CdSe/CdS/ZnS and CdSe/ZnS core/shell QDs to TiO_2 films can be significantly enhanced after thermal annealing at temperature ranging from 100 °C to 300 °C. The operation of QDSSCs involves the two recombination mechanisms as follows: (i) loss of electrons that are transferred to the TiO_2 and (ii) loss of electrons at the QD–electrolyte interface or QD trap states prior to their transfer to the TiO_2. The latter influences the effective charge separation efficiency in QDSSCs [6]. It is well known that the electron transfer rate (efficiency) is strongly dependent on the distance between the CdSe QDs to TiO_2. Recently Zhu et al. studied the rates of charge separation from CdSe/ZnS core/multishell QDs to anthraquinone as a function of the ZnS shell thickness by

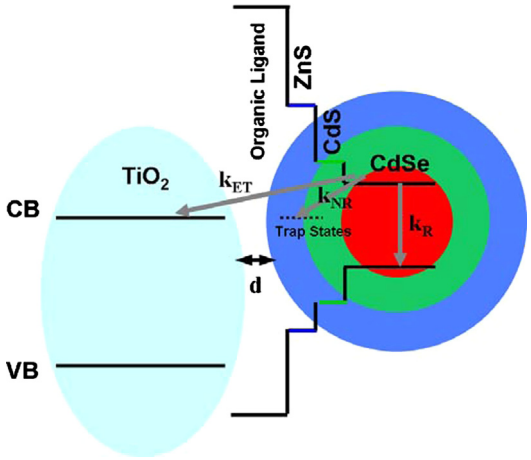

Fig. 8. Schematic diagram of electronic levels of CdSe/CdS/ZnS core/multishell QDs and TiO_2 film. The gray arrowheads represent the rate k_{ET} of electron transfer from CdSe QDs to TiO_2, the rate k_{NR} of the nonradiative recombination at the surface/interface trap states, and the rate k_R of the exciton recombination. The black line d with double arrowheads shows the distance between the QDs and the TiO_2 film.

transient absorption spectroscopy [37]. In this experiment, dodecanthiol ligands ($CH_3(CH_2)_{11}SH$) were still covered on the surface of the CdSe QDs after purification for several times by the mixture of chloroform and acetone. Some of the ligands can be removed after heat treatment at high temperatures. Therefore, as shown in Fig. 8, the removal of ligands on the QD surface can effectively decrease the distance between the CdSe core and TiO_2 films and consequently enhance the photoinduced electron transfer between them via heat treatment [18,32,37]. Based on Marcus's theory, the green QDs with a smaller core and a thinner multishell should have a higher rate of the electron transfer than that of the red QDs with a bigger core and a thicker multishell [8–11]. In addition, we find that the electron transfer rate of the green QDs is really smaller than that of the red QDs. This might be because the existence of the surface defect/trap state emissions with relative long lifetimes and the difference in the amount of ligands on the QD surface disturb the accurate determination of the electron transfer rate. Therefore, the experimental results have demonstrated that thermal annealing treatment on ZnS or CdS/ZnS shell coated CdSe QDs can result in a significant enhancement in rate and efficiency of electron transfer, which is consistent with an improvement in performances of TiO_2/CdSe QD based photovoltaic devices [12–16,22–28]. We can make more intimately contact CdSe QDs with TiO_2 films, thus facilitating electron transfer from the QDs to the conduction band of TiO_2 films. The more significant enhancement of the electron transfer from CdSe QDs to the metal oxides can be realized by effectively removing the ligands on the QD surface through annealing treatment.

On the other hand, as seen in Fig. 8, the trap states as non-radiative recombination centers on the surface of CdSe core QDs can be effectively passivated by using an inorganic shell and organic ligands to improve the PL quantum yield of the QDs [34]. However, large amount of non-radiative recombination centers on the surface of QDs may appear again due to desorption or loss of the ligands or degradation of the shell after thermal annealing, dramatically quenching the PL quantum yield of QDs and causing a decrease in generation efficiency of excitons in the QDs [29–33]. In our experiment, the electron transfer rate and efficiency have been significantly enhanced for the CdSe/ZnS core/shell QDs with supper thermal- and photo-stability although a small degradation is confirmed in the yellow CdSe/ZnS core/shell QDs due to the formation of surface defect/trap states during thermal annealing. However, it was noted that naked CdSe core

QDs onto TiO_2 and SiO_2 films could not be well studied to explore the effect of thermal annealing on the electron transfer because the PL quantum yield of the QDs in solution was very low below 5% after the purification and further the PL properties of the QDs annealed at high temperatures were greatly degraded due to the loss of ligands on the surface of the QDs, which is similar to that observed in CdSe core QD films reported recently [32]. Therefore, it is necessary to control the formation of surface defect/trap states in QDs as non-radiative recombination centers during post heat treatment by using an optimized shell structure to realize the maximum electron transfer rate and efficiency in the metal oxide/QD systems with good thermal- and photo-stability.

4. Conclusions

In summary, we have studied the effect of thermal annealing on electron transfer from CdSe core/shell QDs to TiO_2 films. It is found that the CdSe core/shell QDs with red, yellow and green emissions exhibit a significant enhancement in electron transfer rate from several times to an order of magnitude after thermal annealing, compared with as-prepared QDs on TiO_2 films. At the same time, the maximum improvement in electron transfer efficiency is also found to reach up to 100%. The enhancement could be explained by the reduced distance between the QDs and TiO_2 via post treatment. In addition, the formation of large amount of surface defect/trap states in QDs as non-radiative recombination centers was found in yellow CdSe/ZnS core/shell QDs perhaps due to the removal of the ligands on the surface of QDs during the annealing process based on the decrease in PL lifetime of the QDs. The relaxation processes of carriers into the trap states provide potentially detrimental recombination pathways, resulting in the degradation of QD based optoelectronic devices. The electron transfer rate and efficiency are expected to be further improved by using ligand molecules that can be easily removed to effectively reduce the QD–TiO_2 distance via thermal annealing. Therefore, the thermal annealing treatment is an effective tool to enhance the electron transfer processes from core/shell QDs to TiO_2 films for further improvement in performances of QD based optoelectronic devices.

Acknowledgments

This work was supported by the Hundred Talent Program of the Chinese Academy of Sciences and the National Natural Science Foundation of China (Nos. 60976049, 51102227, 11274304, and 61275047). J.Z. thanks Prof. Peng Wang for his helpful discussion.

References

[1] W.U. Huynh, J.J. Dittmer, A.P. Alivisatos, Science 295 (2002) 2425.
[2] P.V. Kamat, J. Phys. Chem. C 112 (2008) 18737.
[3] D.V. Talapin, J.S. Lee, M.V. Kovalenko, E.V. Shevchenko, Chem. Rev. 110 (2010) 389.
[4] A.J. Nozik, M.C. Beard, J.M. Luther, M. Law, R.J. Ellingson, J.C. Johnson, Chem. Rev. 110 (2010) 6873.
[5] J.B. Sambur, T. Novet, B.A. Parkinson, Science 330 (2010) 63.
[6] I. Mora-Sero, J. Bisquert, J. Phys. Chem. Lett. 1 (2010) 3046.
[7] F. Hetsch, X.Q. Xu, H.K. Wang, S.V. Kershaw, A.L. Rogach, J. Phys. Chem. Lett. 2 (2011) 1879.
[8] I. Robel, V. Subramanian, M. Kuno, P.V. Kamat, J. Am. Chem. Soc. 128 (2006) 2385.
[9] I. Robel, M. Kuno, P.V. Kamat, J. Am. Chem. Soc. 129 (2007) 4136.
[10] A. Kongkanand, K. Tvrdy, K. Takechi, M. Kuno, P.V. Kamat, J. Am. Chem. Soc. 130 (2008) 4007.
[11] K. Tvrdy, P.A. Frantsuzov, P.V. Kamat, Proc. Natl. Acad. Sci. 108 (2011) 29.
[12] Q. Shen, J. Kobayashi, L.J. Diguna, T. Toyoda, J. Appl. Phys. 103 (2008) 084304.
[13] S. Gimenez, I. Mora-Sero, L. Macor, N. Guijarro, T. Lana-Villarreal, R. Gomez, L.J. Diguna, Q. Shen, T. Toyoda, J. Bisquert, Nanotechnology 20 (2009) 295204.
[14] N. Guijarro, J.M. Campina, Q. Shen, T. Toyoda, T. Lana-Villarreal, R. Gomez, Phys. Chem. Chem. Phys. 13 (2011) 12024.
[15] I. Mora-Sero, S. Gimenez, F. Fabregat-Santiago, R. Gomez, Q. Shen, T. Toyoda, J. Bisquert, Acc. Chem. Res. 42 (2009) 1848.
[16] Z.J. Ning, H.N. Tian, H.Y. Qin, Q. Zhang, H. Ågren, L.C. Sun, Y. Fu, J. Phys. Chem. C 114 (2010) 15184.
[17] J.B. Sambur, B.A. Parkinson, J. Am. Chem. Soc. 132 (2010) 2130.
[18] V.J. Porter, S. Geyer, J.E. Halpert, M.A. Kastner, M.G. Bawendi, J. Phys. Chem. C 112 (2008) 2308.
[19] E. Talgorn, R.D. Abellon, P.J. Kooyman, J. Piris, T.J. Savenije, A. Goossens, A.J. Houtepen, L.D.A. Siebbeles, ACS Nano 4 (2010) 1723.
[20] J.S. Lee, M.V. Kovalenko, J. Huang, D.S. Chung, D.V. Talapin, Nat. Nanotechnol. 6 (2011) 348.
[21] S.Y. Jin, T.Q. Lian, Nano Lett. 9 (2009) 2448.
[22] W.U. Huynh, J.J. Dittmer, W.C. Libby, G.L. Whiting, A.P. Alivisatos, Adv. Funct. Mater. 13 (2003) 73.
[23] Y.H. Niu, A.M. Munro, Y.J. Cheng, Y.Q. Tian, M.S. Liu, J.L. Zhao, J.A. Bardecker, I.J.L. Plante, D.S. Ginger, A.K.Y. Jen, Adv. Mater. 19 (2007) 3371.
[24] Q.J. Sun, G. Subramanyam, L.M. Dai, M. Check, A. Campbell, R. Naik, J. Grote, Y.Q. Wang, ACS Nano 3 (2009) 737.
[25] C.Y. Liu, Z.C. Holman, U.R. Kortshagen, Adv. Funct. Mater. 20 (2010) 2157.
[26] C.F. Chi, S.Y. Liau, Y.L. Lee, Nanotechnology 21 (2010) 025202.
[27] M. Drndic, M.V. Jarosz, N.Y. Morgan, M.A. Kastner, M.G. Bawendi, J. Appl. Phys. 92 (2002) 7498.
[28] M. Law, J.M. Luther, Q. Song, B.K. Hughes, C.L. Perkins, A.J. Nozik, J. Am. Chem. Soc. 130 (2008) 5974.
[29] H.J. Choi, S.J. Wang, H. Kim, H.H. Park, H.J. Chang, H. Jeon, Appl. Surf. Sci. 254 (2008) 6886.
[30] U. Farva, C. Park, Sol. Energy Mater. Sol. Cells 94 (2010) 303.
[31] A.T. Fafarman, W. Koh, B.T. Diroll, D.K. Kim, D. Ko, S.J. Oh, X.C. Ye, V. Doan-Nguyen, M.R. Crump, D.C. Reifsnyder, C.B. Murray, C.R. Kagan, J. Am. Chem. Soc. 133 (2011) 15753.
[32] Y.Q. Zhang, X.A. Cao, Appl. Phys. Lett. 99 (2010) 023106.
[33] S. Biswas, D.J. Gosztola, G.P. Wiederrecht, M.A. Stroscio, M. Dutta, J. Electron. Mater. 41 (2012) 524.
[34] R.G. Xie, U. Kolb, J. Li, T. Basche, A. Mews, J. Am. Chem. Soc. 127 (2005) 7480.
[35] D.C. Pan, N.N. Zhao, Q. Wang, S.C. Jiang, X.L. Ji, L.J. An, Adv. Mater. 17 (2005) 1991.
[36] W. Stober, A. Fink, E. Bohn, J. Colloid Interface Sci. 26 (1968) 62.
[37] H.M. Zhu, N.H. Song, T.Q. Lian, J. Am. Chem. Soc. 132 (2010) 15038.